J. Fluid Mech. (1978), *vol.* 87, *part* 2, *pp.* 243–261
Printed in Great Britain

Magnetic flux ropes and convection

By D. J. GALLOWAY,
Astronomy Centre, University of Sussex, Brighton, England

M. R. E. PROCTOR AND N. O. WEISS
Department of Applied Mathematics and Theoretical Physics,
University of Cambridge, England

(Received 4 November 1977)

Three-dimensional cellular convection concentrates magnetic flux into ropes when the magnetic Reynolds number is large. Amplification of the magnetic field is limited by the Lorentz force and the maximum field in a flux rope can be estimated. Boundary-layer analysis yields a completely self-consistent solution for a model of convection driven by imposed horizontal temperature gradients, and the transition from a kinematic to a dynamic regime can be followed in detail. The maximum value of the amplified field is proportional to the square root of the ratio of the viscous to the magnetic diffusivity.

1. Introduction

The interaction between magnetic fields and cellular convection is actually observed in the sun, where photospheric granules concentrate the flux into regions with intense local magnetic fields. Such flux ropes are likely to be formed in any stellar or planetary dynamo that is driven by convection. When the total flux is small concentration is limited by diffusion but stronger fields exert forces which oppose the concentration. In this paper we establish that the amplified magnetic field reaches a maximum during the transition from a kinematic to a dynamic regime and find the value of this maximum.

We consider convection in an electrically conducting Boussinesq fluid with an externally imposed magnetic field. In the kinematic regime the Lorentz force is negligible and the magnetic field is determined by the induction equation. For persistent convection with a typical velocity U and length scale L, the magnetic Reynolds number

$$R_m = UL/\eta, \tag{1.1}$$

where η is the magnetic diffusivity. If $R_m \gg 1$ magnetic flux is eventually expelled from the convective eddies and concentrated into ropes between them (Parker 1963; Clark 1965, 1966; Weiss 1966, 1977; Clark & Johnson 1967; Busse 1975); for three-dimensional flow the peak field in the ropes

$$B^* \sim R_m B_0, \tag{1.2}$$

where B_0 is the average field in the absence of motion. If B_0 is sufficiently large the Lorentz force can no longer be neglected; in this dynamic regime the induction equation is coupled to the equation of motion and they must be solved together.

Nonlinear magnetoconvection has been studied in two idealized configurations. In the Oberbeck problem convection is driven in a plane layer by maintaining horizontal temperature gradients at, say, its lower boundary; in the Rayleigh–Bénard problem motion is produced by an imposed vertical temperature gradient. Busse (1975) showed for weak two-dimensional Rayleigh–Bénard convection that B^* could increase without limit if the ratio of the viscous to the magnetic diffusivity was sufficiently large. This result has been confirmed by numerical experiments on two-dimensional convection (Peckover & Weiss 1978; Weiss 1975) and on axisymmetric convection in a cylindrical cell (Galloway & Moore 1978). These computations refute the old conjecture that B^* is limited by the equipartition field

$$B_e = (\mu\rho)^{\frac{1}{2}} U, \tag{1.3}$$

where μ is the permeability and ρ the density.

This paper is principally concerned with flux ropes formed by three-dimensional flow converging to an axis. In the next section we formulate an idealized model problem with axisymmetric convection in a cylindrical cell. When R_m is large nearly all the flux is concentrated on the axis. The field generates a counter-flow and when this is of the same order as the original flow towards the axis B^* attains a maximum. A simple one-dimensional treatment is described in § 3. Fortunately the Oberbeck problem is amenable to analysis by boundary-layer theory and matched asymptotic expansions. Provided that both the Reynolds number

$$Re = UL/\nu \tag{1.4}$$

and the Péclet number

$$Pe = UL/\kappa \tag{1.5}$$

are small (where κ and ν are the thermal and viscous diffusivities) a self-consistent solution for the magnetic field, the vorticity and the velocity can be obtained in closed form. The transition from a kinematic to a dynamic regime can be followed exactly and the maximum value of B^* can be calculated. This analysis, which forms the core of the paper, is carried out in § 4. A similar solution for the Rayleigh–Bénard problem, in a restricted parameter range, exhibits interesting features of subcritical convection (Proctor & Galloway 1978); the axisymmetric configuration produces a greater variety of behaviour than the two-dimensional problem studied by Busse (1975). The two-dimensional Oberbeck problem, where flux is concentrated into sheets, is considered briefly in § 5, though it proves less suited to analysis. Finally, we summarize the results and their relevance to astrophysical convection. The maximum value B_m of the peak field B^* in the flux rope is attained when B_0 reaches a critical value that depends only weakly on the applied temperature gradient. For two-dimensional flow this occurs when Ohmic dissipation in the flux rope becomes comparable with viscous dissipation in the convection cell, and

$$B_m^2 \sim (\nu/\eta) B_e^2 / R_m^{\frac{1}{2}}. \tag{1.6}$$

For three-dimensional flow,

$$B_m^2 \sim (\nu/\eta) B_e^2 / \ln R_m \tag{1.7}$$

and Ohmic dissipation does not become important until B_0 is somewhat greater.

2. Formulation of the problem

For steady convection in a Boussinesq fluid the temperature T, the magnetic field $\mathbf{B}$ and the velocity $\mathbf{u}$ satisfy the equations

$$-\mathbf{u}.\nabla T+\kappa\nabla^2 T=0, \tag{2.1}$$

$$\nabla\wedge(\mathbf{u}\wedge\mathbf{B})+\eta\nabla^2\mathbf{B}=0 \tag{2.2}$$

and

$$-\rho_0(\mathbf{u}.\nabla)\mathbf{u}-\nabla P+\rho\mathbf{g}+\mathbf{j}\wedge\mathbf{B}+\rho_0\nu\nabla^2\mathbf{u}=0, \tag{2.3}$$

where

$$\rho=\rho_0[1-\alpha(T-T_0)] \tag{2.4}$$

and

$$\nabla.\mathbf{u}=0, \quad \nabla.\mathbf{B}=0. \tag{2.5}$$

Here ρ_0 and T_0 are constants, $\mathbf{g}$ is the gravitational acceleration and α the coefficient of thermal expansion, while the electric current $\mathbf{j}=\mu^{-1}\nabla\wedge\mathbf{B}$. Taking the curl of (2.3) eliminates the pressure P and yields the equation

$$\nabla\wedge(\mathbf{u}\wedge\boldsymbol{\omega})-\alpha\nabla T\wedge\mathbf{g}+\rho_0^{-1}\nabla\wedge(\mathbf{j}\wedge\mathbf{B})+\nu\nabla^2\boldsymbol{\omega}=0 \tag{2.6}$$

for the vorticity $\boldsymbol{\omega}=\nabla\wedge\mathbf{u}$.

We adopt cylindrical polar co-ordinates (r,ϕ,z) and assume that both the magnetic field and the velocity are purely meridional and symmetric about the vertical (z) axis. Then it is convenient to introduce a Stokes flux function χ and a Stokes stream function ψ such that

$$\mathbf{B}=\frac{1}{r}\left(-\frac{\partial\chi}{\partial z},\,0,\,\frac{\partial\chi}{\partial r}\right), \quad \mathbf{u}=\frac{1}{r}\left(-\frac{\partial\psi}{\partial z},\,0,\,\frac{\partial\psi}{\partial r}\right), \tag{2.7}$$

while the electric current and vorticity are purely azimuthal, so that

$$j\equiv|\mathbf{j}|=-(\mu r)^{-1}D^2\chi, \quad \omega\equiv|\boldsymbol{\omega}|=-r^{-1}D^2\psi, \tag{2.8}$$

where the Stokes operator

$$D^2\equiv r\frac{\partial}{\partial r}\left(\frac{1}{r}\frac{\partial}{\partial r}\right)+\frac{\partial^2}{\partial z^2}. \tag{2.9}$$

Then (2.1), (2.2) and (2.6) reduce to

$$\frac{1}{r}\frac{\partial(T,\psi)}{\partial(r,z)}+\kappa\nabla^2 T=0, \quad \frac{1}{r}\frac{\partial(\chi,\psi)}{\partial(r,z)}+\eta D^2\chi=0 \tag{2.10), (2.11}$$

and

$$\frac{\partial(\omega/r,\psi)}{\partial(r,z)}-\frac{1}{\rho_0}\frac{\partial(j/r,\chi)}{\partial(r,z)}-g\alpha\frac{\partial T}{\partial r}+\frac{\nu}{r}D^2(r\omega)=0. \tag{2.12}$$

We consider convection within the cylinder $\{0\leqslant r\leqslant r_0;\,0\leqslant z\leqslant d\}$ and assume the simplest boundary conditions. The normal velocity and the tangential stress vanish on all the boundaries, the total flux is fixed and equal to that for a uniform vertical field B_0, while the tangential Maxwell stress vanishes at $z=0,\,d$. Hence the radial component of $\mathbf{B}$ is zero on all the boundaries, though field lines are free to move along the horizontal boundaries. Thus

$$\psi=0, \quad \omega=0 \quad (r=0,r_0;z=0,d), \tag{2.13a}$$

$$\chi=0 \quad (r=0), \quad \chi=\tfrac{1}{2}B_0r_0^2 \quad (r=r_0), \quad \partial\chi/\partial z=0 \quad (z=0,d). \tag{2.13b}$$

We assume that the temperature is prescribed on the upper and lower boundaries and that there is no heat flow across the curved cylindrical boundary, so that

$$T = T_0 \quad (z = d), \quad T = T_0 + \Delta T\tau(r) \quad (z = 0), \tag{2.14a}$$

$$\partial T/\partial r = 0 \quad (r = 0, r_0), \tag{2.14b}$$

where ΔT is a measure of the imposed temperature difference. For the Oberbeck problem τ is some prescribed function of order unity such that $d\tau/dr = 0$ at $r = r_0$; for the Rayleigh–Bénard problem $\tau = 1$. Let L be a typical length scale, related to the depth or radius of the convection cell. Then a particular configuration is defined by four dimensionless parameters: the Rayleigh number

$$R = g\alpha\Delta T L^3/\kappa\nu, \tag{2.15}$$

the Chandrasekhar number $$Q = B_0^2 L^2/\mu\rho\eta\nu, \tag{2.16}$$

which is the square of the Hartmann number, the Prandtl number

$$p_1 = \nu/\kappa \tag{2.17}$$

and the magnetic Prandtl number $$p_2 = \nu/\eta. \tag{2.18}$$

It is also convenient to define a further ratio

$$p_3 = p_2/p_1 = \kappa/\eta. \tag{2.19}$$

In most of the ensuing discussion we shall assume that $\kappa \gg \eta$ ($p_3 \gg 1$) in order that any thermal boundary layers will be much thicker than the corresponding magnetic layers. In addition it is technically convenient to assume that $p_2 \gg 1$, so that $Re = O(1)$ and there are no viscous boundary layers. The first assumption holds for laminar flow in many stellar situations, though the second is unrealistic; it is not obvious how the corresponding turbulent diffusivities should be calculated.

3. The central flux rope

The nonlinear equations (2.10)–(2.12) are analytically intractable, though they have been solved numerically for the Rayleigh–Bénard problem (Galloway 1977; Galloway & Moore 1978). The results of these numerical experiments may be summarized as follows. In the kinematic regime, when the magnetic torque in (2.12) is small, flux is expelled from most of the convecting region and concentrated at the axis and periphery of the cell. To fix the magnetic Reynolds number, defined by (1.1), we choose U to be the maximum vertical velocity at the axis and L to be the radius r_0, which is of the same order as the depth d. For $R_m \gg 1$ nearly all the flux is contained in a rope of radius $\epsilon r_0 (\epsilon \ll 1)$ at the axis, where $\epsilon \sim R_m^{-\frac{1}{2}}$. The field has a Gaussian profile and its peak value $B^* \sim B_0/\epsilon^2$. As B_0 is increased (holding R constant) the Lorentz force generates vorticity with the opposite sense to that produced by the buoyancy force, and so reduces the radial inflow towards the axis. Figure 1 shows an example of the streamlines and lines of force in the dynamic regime. Magnetic flux is expelled from the toroidal eddy and the motion is excluded from the central flux rope. However, the velocity is affected only in a narrow region around the axis and the convective heat transport is scarcely changed. For yet larger values of B_0 the flux rope expands until it fills the cell and convection is ultimately suppressed.

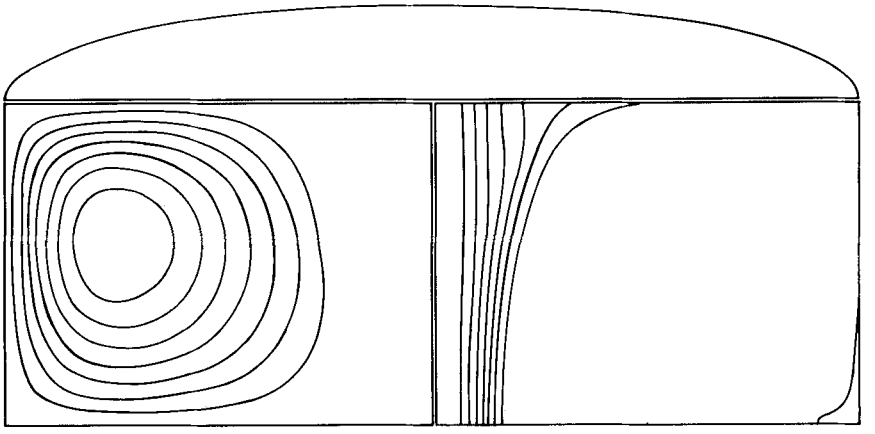

(*a*) (*b*)

FIGURE 1. (*a*) Streamlines and (*b*) lines of force for the Rayleigh–Bénard problem in the dynamic regime. For this case $R = 13150$, $Q = 100$, $p_1 = 1$, $p_3 = 10$ and the radius-to-depth ratio is $\frac{4}{3}$.

We can show analytically that, provided that the magnetic Reynolds number is large, flux is concentrated almost entirely at the axis of the cell, both in the kinematic and in the dynamic regime. The induction equation (2.11) can be expressed in the form

$$\nabla . [r^2 \nabla (\chi / r^2] = \eta^{-1} \nabla . [\chi \mathbf{u}]. \tag{3.1}$$

Integrating this equation over the volume of the cell and applying the divergence theorem, we find that

$$\int r^2 \nabla \left(\frac{\chi}{r^2}\right) . d\mathbf{S} = 2\pi r_0 \int \left[\frac{\partial \chi}{\partial r} - \frac{2\chi}{r}\right]_{r=r_0} dz = 0, \tag{3.2}$$

since both $\partial\chi/\partial z$ and the normal velocity vanish on the boundaries. Now the average field on the outer boundary is

$$\bar{B} = \frac{1}{r_0 d} \int_0^d \frac{\partial \chi}{\partial r}\bigg|_{r=r_0} dz \tag{3.3}$$

and the total flux through the cylinder $\pi r_0^2 B_0 = 2\pi\chi(r_0, z)$. Hence, from (3.2),

$$\bar{B} = B_0, \tag{3.4}$$

i.e. in a steady state the average field at the outer boundary is unaffected by the motion (provided that the radial component of the field vanishes at $z = 0, d$). This remarkable result can be extended to fields with azimuthal components too but does not hold unless the field is axisymmetric; some related arguments were advanced by, for example, Spitzer (1957). In a rotating fluid, conservation of angular momentum yields an equation analogous to (3.1). The vorticity behaves like a magnetic field and the corresponding result is obvious.

From (3.4) it follows that nearly all the magnetic flux is concentrated into a rope at the axis. For $R_m \gg 1$ the magnetic field vanishes except in the immediate vicinity of streamlines that meet the boundary (cf. Batchelor 1956). At these streamlines ropes or sheets are formed. Thus flux is concentrated either into a central column or into a sheet at the outer boundary or into a sheet separating two adjacent eddies.

We assume that the region $\{0 \leqslant r \leqslant r_0\}$ is occupied by a single eddy. Then if R_m is sufficiently large the field must be confined to boundary layers at $r = 0$, r_0. At the centre there will be a rope of radius ϵr_0 while at the periphery there will be an annular region with thickness of order ϵr_0, where $\epsilon \sim R_m^{-\frac{1}{2}}$ (cf. Weiss 1966). The fraction of the total flux contained in the outer annulus is of order $\epsilon r_0^2 \bar{B}/r_0^2 B_0 \sim R_m^{-\frac{1}{2}}$. As $R_m \to \infty$ this fraction becomes negligible. Nearly all the flux is therefore concentrated into a central flux rope with radius of order $R_m^{-\frac{1}{2}} r_0$ and a field $B^* \sim R_m B_0$.

We next have to consider the effect of this flux rope on convection. The behaviour of the numerical solutions suggests that the transition from a kinematic to a dynamic regime can be investigated by boundary-layer techniques. Moreover, nonlinear advection of vorticity does not seem to be important for this problem (Jones, Moore & Weiss 1976; Peckover & Weiss 1978). We shall assume therefore that $p_1 \gg 1$, so that the Reynolds number $Re \ll 1$ and the first term in (2.12) may be ignored. Although our treatment is formally valid only for small Re we expect that the form of our asymptotic results will hold for high Reynolds numbers too.

Equation (2.12) can be rewritten as

$$\frac{1}{r} D^2 (r\omega) = \frac{g\alpha}{\nu} \frac{\partial T}{\partial r} - \frac{1}{\rho_0 \nu} \mathbf{B} \cdot \nabla j. \tag{3.5}$$

This equation is linear in ω: the vorticity is generated by the two source terms on the right-hand side, which may be considered separately. The radial temperature gradient produces an eddy with velocity $\mathbf{u}_0$ and vorticity ω_0, while the magnetic torque drives a counter-rotating eddy with velocity $\mathbf{u}_1$ and vorticity ω_1, where

$$\frac{1}{r} D^2(r\omega_0) = \frac{g\alpha}{\nu} \frac{\partial T}{\partial r}, \quad \frac{1}{r} D^2(r\omega_1) = -\frac{1}{\rho_0 \nu} \mathbf{B} \cdot \nabla j. \tag{3.6}$$

The transition from a kinematic to a dynamic regime occurs as $|\mathbf{u}_1|$ becomes comparable to $|\mathbf{u}_0|$ on the axis. From figure 1 it is clear that the magnetic torque can be regarded as concentrated in a current sheath of radius ϵr_0 about the axis and the left-hand side of (3.6*b*) is dominated by the radial derivatives; on the right-hand side

$$\mathbf{B} \cdot \nabla j \sim \frac{B^* j}{d} \sim -\frac{B^{*2}}{\mu d} \delta(r - \epsilon r_0). \tag{3.7}$$

As a preliminary to the boundary-layer analysis in § 4 we consider a one-dimensional model in which all vertical variations are ignored. This simple problem can readily be solved to yield the asymptotic behaviour of the field.

For the one-dimensional problem it is convenient to take r_0 as the unit of length. In the rest of this section we use a dimensionless radius $r' = r/r_0$ and suppress the prime. Vorticity is generated by the thermal plumes at the axis and periphery of the cell. We suppose that $\kappa \gg \eta$, so that the temperature variation has a scale much greater than ϵ, and that the thermal field produces a vertical velocity $V_0(r)$ with $V_0(0) = U > 0$. Let the Lorentz force drive a vertical velocity $V_1(r)$. To calculate V_1 we first obtain the Green's function $\omega(r)$ that satisfies

$$\frac{d}{dr}\left\{\frac{1}{r}\frac{d}{dr}(r\omega)\right\} = \delta(r - \epsilon) \tag{3.8}$$

then find the corresponding velocity $v(r)$ and stream function $\psi(r)$ such that $\omega = -dv/dr$ and $v = r^{-1}d\psi/dr$. From (2.13) the appropriate boundary conditions are

$$\psi(0) = \psi(1) = 0, \quad \omega(0) = \omega(1) = 0. \tag{3.9}$$

This problem can readily be solved. At the axis the velocity

$$V \equiv v(0) = -\tfrac{1}{2}\epsilon^2[|\ln\epsilon| - \tfrac{1}{4}(1-\epsilon^2)] \doteqdot -\tfrac{1}{2}\epsilon^2|\ln\epsilon| \tag{3.10}$$

when $\epsilon \ll 1$. Then

$$v(r) \doteqdot \begin{cases} V\left(1 - \dfrac{r^2}{2\epsilon^2|\ln\epsilon|}\right) & (0 \leqslant r \leqslant \epsilon), \quad (3.11a) \\ -\dfrac{V}{|\ln\epsilon|}\left[\ln r + \tfrac{1}{2}(\tfrac{3}{2} - r^2) + \dfrac{\ln r}{4|\ln\epsilon|}\right] & (\epsilon \leqslant r \leqslant 1), \quad (3.11b) \end{cases}$$

while the vorticity

$$\omega(r) \doteqdot \begin{cases} \dfrac{V}{|\ln\epsilon|}\dfrac{(1-\epsilon^2)}{\epsilon^2} r & (0 \leqslant r \leqslant \epsilon), \quad (3.12a) \\ \dfrac{V}{|\ln\epsilon|}\dfrac{(1-r^2)}{r} & (\epsilon \leqslant r \leqslant 1), \quad (3.12b) \end{cases}$$

where the higher-order terms are retained to ensure continuity at $r = \epsilon$. This simplified analysis shows that the maximum vorticity

$$\omega^* \doteqdot V/\epsilon|\ln\epsilon| \tag{3.13}$$

occurs at $r = \epsilon$. The corresponding velocity extends across the entire cell and reverses its direction only near the centre, for $v(r) = 0$ when $r \doteqdot 0{\cdot}55$. However, examination of (3.11) reveals that v is small unless $r \lesssim \epsilon$: for instance $v(1) \doteqdot V/(4|\ln\epsilon|) \ll V$. Thus a localized current distribution, like that in (3.7), drives a velocity which is strongly concentrated near the axis, provided that $|\ln\epsilon| \gg 1$. This important logarithmic term appears because the axis is a singular point and it cannot be derived by any simple dimensional argument.

Kinematic amplification is halted when $|V_1(0)|$ is comparable with U. We shall later confirm that this corresponds to a local maximum of the field B^* in the flux rope. The maximum value B_m of B^* can be estimated as follows. At the axis the dimensionless Lorentz force generates a velocity

$$V_1(0) \sim \frac{B^{*2}}{\mu\rho_0\nu} V \sim -\epsilon^2|\ln\epsilon|\frac{B^{*2}}{\mu\rho_0\nu}, \tag{3.14}$$

from (3.6*b*), (3.7) and (3.10). Hence

$$B_m^2 \sim \mu\rho_0\nu U/\epsilon^2|\ln\epsilon|. \tag{3.15}$$

Now $\epsilon \sim R_m^{-\frac{1}{2}}$ and so, provided that $\ln R_m \gg 1$,

$$B_m^2 \sim \frac{\mu\rho_0 U^2}{\ln R_m}\left(\frac{\nu}{\eta}\right) = \frac{1}{\ln R_m} p_2 B_e^2. \tag{3.16}$$

The corresponding value of the imposed field B_0 satisfies

$$B_0^2 \sim (\eta/U)^2 B_m^2 \sim \mu\rho_0 \nu\eta/\ln R_m, \tag{3.17}$$

so that B^* is a maximum when $\quad Q \sim 1/\ln R_m.$ (3.18)

Thus the value of Q for which the concentrated field is a maximum depends only weakly on the Rayleigh number, through the logarithm in the denominator. These results have been derived for a top-hat profile of the magnetic field in the flux rope but the Green's function of (3.12) could be used to calculate B_m for a Gaussian profile and (3.16) would be unaffected. Instead of pursuing this we shall solve an axisymmetric problem properly in the next section.

4. A boundary-layer analysis of the Oberbeck problem

4.1. *The model*

In this section we present a model of magnetic convection which permits an analytical description of the structure of the flux rope. The principal simplifying assumption is that this flux rope is 'thin'. The model yields an explicit expression for the peak field over a wide range of values of the magnetic flux, as well as a quantitative description of the transition from a kinematic to a nonlinear dynamic regime. These results provide some justification for the one-dimensional theory discussed in § 3.

We shall investigate the Oberbeck problem defined in § 2. We suppose that the Péclet number Pe is vanishingly small and that the Reynolds number $Re \ll 1$ but that the magnetic Reynolds number $R_m \gg 1$; these assumptions imply that $p_2, p_3 \gg 1$. Then the temperature field is unaffected by the motion and the nonlinear inertial term can be neglected in (2.12). In the kinematic regime there is a basic flow which concentrates the magnetic field in a flux rope on the axis; from (2.12) the characteristic speed U is proportional to the horizontal temperature gradient at the base of the cylinder, so that

$$U \sim g\alpha\Delta T r_0^2/\nu. \tag{4.1}$$

In the dynamic regime this flow is modified by the magnetic field. To study this process we use boundary-layer theory and the method of matched asymptotic expansions. The analysis is rendered tractable by the geometrical structure of the rope; the axis is a singular point of the equations and this makes all the difference between axisymmetric and two-dimensional magnetoconvection.

We consider the interior of a cylinder of radius $r_0 = L\gamma$, where γ is a prescribed constant of order unity introduced for subsequent convenience (see § 4.5 below). A temperature $T_b = T_0 + \Delta T\tau(r/L)$ is prescribed at $z = 0$; τ is so chosen that fluid rises at the axis and $d\tau/dr = 0$ at $r = r_0$ but can otherwise be quite general. Since the thermal diffusivity is large the temperature field in the cylinder satisfies

$$\nabla^2 T = 0, \tag{4.2a}$$

$$\partial T/\partial r = 0 \quad (r = r_0), \quad T = T_0 \quad (z = d), \quad T = T_b \quad (z = 0) \tag{4.2b}$$

[cf. (2.10) and (2.14)]. This equation is solved by some axisymmetric temperature

$$T(r, z) = T_0 + \Delta T\theta(r/L, z/L), \tag{4.3}$$

where θ depends on τ. If this temperature distribution is substituted into the vorticity equation (2.12) and the equations are non-dimensionalized by writing

$$(r,z) = L(r',z'), \quad d = Ld', \quad \mathbf{u} = (g\alpha\Delta TL^2/\nu)\,\mathbf{u}', \quad \mathbf{B} = B_0\mathbf{B}', \tag{4.4}$$

we obtain (after dropping primes) the system

$$\frac{\partial\theta}{\partial r} + QR_m^{-1}\frac{\partial(\chi, r^{-2}D^2\chi)}{\partial(r,z)} = r^{-1}D^2(r\omega), \tag{4.5a}$$

$$\mathbf{u}\,.\,\nabla\chi = R_m^{-1}D^2\chi. \tag{4.5b}$$

The magnetic Reynolds number is now an external parameter given by

$$R_m = g\alpha\Delta TL^3/\nu\eta \tag{4.6}$$

and Q is supposed to be of order unity. Precise bounds on Q that ensure the validity of the analysis will be given below in § 4.4.

When $R_m \gg 1$ we may approach the problem by noting that the magnetic field is confined to a thin flux rope at the axis, with thickness of order $R_m^{-\frac{1}{2}}$. The structure of the rope can be obtained exactly (to leading order in R_m) for any velocity field in the cell; the solution can then be used to find the vorticity generated in the rope by the Lorentz force, and thus the modification to the basic flow caused by the rope's presence. We can then obtain an analytical expression for the magnetic field as a function of Q and R_m. Use of the principle of matched asymptotic expansions leads us to distinguish between an 'inner solution' (the rope) described in terms of the stretched variable

$$\xi = R_m^{\frac{1}{2}}r \tag{4.7}$$

and an 'outer solution' where the field is negligible and all length scales are of order unity.

4.2. *The inner solution*

It is convenient to separate the velocity field $\mathbf{u}$ into two parts, as was done in § 3. We set $\psi = \psi_0 + \psi_1$, where, from (2.8) and (4.5*a*), ψ_0, the stream function of the basic flow, satisfies

$$r^{-1}D^2(D^2\psi_0) = -\partial\theta/\partial r \tag{4.8}$$

with the appropriate boundary conditions (2.13*a*), while ψ_1 describes the velocity field due to the Lorentz force alone, so that

$$r^{-1}D^2(D^2\psi_1) = -QR_m^{-1}\partial(\chi, r^{-2}D^2\chi)/\partial(r,z). \tag{4.9}$$

The simplicity of this separation derives from the neglect of the inertial forces. It can be shown, though, that a similar qualitative picture appears even for Re of order unity. Note that this separation cannot be achieved in (4.5*b*) since the sum $\mathbf{u}_0 + \mathbf{u}_1$ appears there as a *coefficient* in the equation, thereby giving the problem its nonlinear character. We now suppose that near the axis $r = 0$ the stream function $\psi(r,z) \sim \frac{1}{2}r^2f(z) + o(r^2)$ and that $f(z)$ is of order unity; this implies a (very modest) restriction on Q which will be given later. Thus $f(z)$ is the vertical velocity at the axis, and as before we set

$f = f_0 + f_1$, where f_0 is known from (4.8). From (2.13), $f(0) = f''(0) = 0$. Rewriting (4.5*b*) in terms of ξ, and retaining only terms of leading order in $R_m^{-\frac{1}{2}}$, we obtain

$$\xi \frac{\partial}{\partial \xi}\left(\frac{1}{\xi}\frac{\partial \chi}{\partial \xi}\right) = f\frac{\partial \chi}{\partial z} - \frac{1}{2}\frac{df}{dz}\xi\frac{\partial \chi}{\partial \xi} \tag{4.10}$$

together with the boundary conditions

$$\chi = 0 \quad (\xi = 0), \tag{4.11a}$$

$$\chi \to \chi_0 = \tfrac{1}{2}\gamma^2 \quad (\xi \to \infty), \tag{4.11b}$$

$$\partial\chi/\partial z = 0 \quad (z = 0). \tag{4.11c}$$

Conditions (4.11*a*, *b*) imply that all the flux is concentrated in the rope, as proved in § 3. The boundary condition at $z = d$ cannot be satisfied by this equation, since $f(d) = 0$ and the flux rope spreads out to fill the cell (cf. figure 1). There is in fact a horizontal boundary layer at $z = d$ produced by the radial outflow, which allows the flux lines to emerge vertically from the cell. However, the vorticity generated in this layer is small compared with that produced by the rope on the axis. We may therefore ignore the upper boundary layer: the unique solution of the parabolic equation (4.10) subject to the boundary conditions (4.11) is then

$$\chi(\xi, z) = \chi_0[1 - \exp(-\tfrac{1}{2}q^2)], \tag{4.12}$$

where

$$q = \xi p^{\frac{1}{2}}, \quad p(z) \equiv f/2z, \tag{4.13}$$

which is valid as long as $d - z \gg R_m^{-\frac{1}{2}}$. Thus the flux rope is Gaussian in cross-section throughout its length. The important function $p(z)$ is directly related to the magnetic field B^* on the axis, since

$$B^*(z) \equiv B_z|_{r=0} = B_0 R_m \left(\frac{1}{\xi}\frac{\partial \chi}{\partial \xi}\right)\Big|_{\xi=0} = B_0 R_m \chi_0 p(z). \tag{4.14}$$

We may now use the solution (4.12) to calculate the vorticity distribution in the flux rope, and thus to find a matching condition that relates the inner to the outer solution. The magnetically induced vorticity ω_1 may be separated into inner and outer functions by writing

$$\omega_1 = \begin{cases} \tilde{\omega}(\xi, z) & \text{(inner)}, \quad (4.15a) \\ \hat{\omega}(r, z) & \text{(outer)}, \quad (4.15b) \end{cases}$$

with the boundary conditions

$$\tilde{\omega} \to 0 \quad (\xi \to 0), \quad \hat{\omega} = 0 \quad (r = \gamma), \tag{4.16a, b}$$

$$\lim_{\xi \to \infty} \tilde{\omega} = \lim_{r \to 0} \hat{\omega}, \tag{4.16c}$$

according to the principle of matched asymptotic expansions. Then, from (3.9), $\tilde{\omega}$ satisfies

$$QR_m^{\frac{1}{2}} \frac{\partial\left(\chi, \frac{1}{\xi}\frac{\partial}{\partial \xi}\left(\frac{1}{\xi}\frac{\partial \chi}{\partial \xi}\right)\right)}{\partial(\xi, z)} = \frac{\partial}{\partial \xi}\left(\frac{1}{\xi}\frac{\partial}{\partial \xi}(\xi\tilde{\omega})\right). \tag{4.17}$$

The Jacobian is easily evaluated from (4.12) and, since z is just a parameter in (4.17), that equation can be rewritten as

$$\frac{\partial}{\partial q}\left(\frac{1}{q}\frac{\partial}{\partial q}(\xi\tilde{\omega})\right) = -2Q\chi_0^2 R_m^{\frac{1}{2}}\frac{dp}{dz}q\exp(-q^2), \tag{4.18}$$

which has the solution

$$r\tilde{\omega} = R_m^{-\frac{1}{2}}\xi\tilde{\omega} = \tfrac{1}{2}Q\chi_0^2[A(z)q^2 + 1 - \exp(-q^2)]\,dp/dz, \tag{4.19}$$

where $A(z)$ is arbitrary. With $r\tilde{\omega}$ given, the boundary-layer stream function $\tilde{\psi}$ is obtained from

$$-r\tilde{\omega} = R_m\xi\frac{\partial}{\partial\xi}\left(\frac{1}{\xi}\frac{\partial\tilde{\psi}}{\partial\xi}\right) \tag{4.20}$$

with the boundary condition $\tilde{\psi} = O(\xi^2)$ as $\xi \to 0$. Clearly $\tilde{\psi}$ will consist of a particular integral $\tilde{\psi}_p$ obtained from (4.20) together with a complementary function

$$\tilde{\psi}_c = \tfrac{1}{2}R_m^{-1}\xi^2 C(z), \tag{4.21}$$

where $C(z)$ is arbitrary. The functions $A(z)$, $C(z)$ and $p(z)$ are determined by considering the outer solution.

4.3. *The outer solution*

Since the magnetic field is negligibly small away from the axis, the equations for $\hat{\omega}$ take the form

$$D^2(r\hat{\omega}) = 0, \tag{4.22a}$$

$$\hat{\omega} = 0 \quad (r = \gamma,\ z = 0, d), \quad \lim_{r\to 0} r\hat{\omega} = \lim_{\xi\to\infty} r\tilde{\omega}. \tag{4.22b, c}$$

It is easily shown that the most general expansion for $r\hat{\omega}$ near $r = 0$ is of the form

$$\begin{aligned} r\hat{\omega} &\sim \alpha(z) + \beta(z)\,r^2\ln r + \gamma(z)\,r^2 + \ldots \\ &\sim \alpha + \beta R_m^{-1}\ln R_m^{\frac{1}{2}}\xi^2 + \beta R_m^{-1}\xi^2\ln\xi + \gamma R_m^{-1}\xi^2 + \ldots . \end{aligned} \tag{4.23}$$

From (4.19), as $\xi\to\infty$ $$r\tilde{\omega} \sim \frac{Q}{2}\chi_0^2\frac{dp}{dz}(1 + A(z)\,p\xi^2 + \ldots). \tag{4.24}$$

Hence for correct matching we must have

$$\alpha(z) = \tfrac{1}{2}Q\chi_0^2\,dp/dz, \tag{4.25a}$$

$$\tfrac{1}{2}AQ\chi_0^2\,p\,dp/dz = -\beta(z)\,R_m^{-1}\ln R_m^{\frac{1}{2}} \tag{4.25b}$$

and, since $\beta = O(\alpha)$, $|A| = O(R_m^{-1}\ln R_m^{\frac{1}{2}})$. Thus A may be neglected at leading order. The dominant behaviour of $r\hat{\omega}$ as $r\to 0$ is thus $r\hat{\omega} \sim \frac{1}{2}Q\chi_0^2 dp/dz$. Near $r = 0$, the stream function $\hat{\psi}$ must satisfy

$$r\hat{\omega} = -D^2\hat{\psi} = \tfrac{1}{2}Q\chi_0^2 dp/dz + o(1), \tag{4.26}$$

which implies that

$$\hat{\psi} = -\frac{Q}{4}\chi_0^2\frac{dp}{dz}r^2\ln r + O(r^2). \tag{4.27}$$

Note that it is not necessary to solve the full elliptic equation for $\hat{\psi}$ to determine its leading-order behaviour near the axis. This is because the complementary function of (4.26), which can be fixed only by reference to the boundary conditions at $r = \gamma$, is

$O(r^2)$ near $r = 0$ and so does not contribute to $\hat{\psi}$ there at leading order. The two-dimensional case is quite different (and much harder) as will be seen in § 5 below.

Hence the limit of the outer solution as $r \to 0$ may be written as

$$\hat{\psi} \sim \frac{1}{4}\frac{dp}{dz}[\xi^2 \ln R_m^{\frac{1}{2}} - \xi^2 \ln \xi] Q\chi_0^2 R_m^{-1}. \tag{4.28}$$

The problem can now be closed by requiring that

$$\lim_{r \to 0} \hat{\psi} = \lim_{\xi \to \infty} \tilde{\psi}. \tag{4.29}$$

From (4.21), $$\tilde{\psi} = \tilde{\psi}_p + \tilde{\psi}_c = \tilde{\psi}_p + \tfrac{1}{2}\xi^2 R_m^{-1} C(z). \tag{4.30}$$

Now $\tilde{\psi}_p$ cannot match the term proportional to $\xi^2 \ln R_m^{\frac{1}{2}}$ since $\ln R_m^{\frac{1}{2}}$ does not appear in the asymptotic expansion for large ξ of the inner solution. Hence $\tilde{\psi}_p$ matches the term proportional to $\xi^2 \ln \xi$ while $\tilde{\psi}_c$ matches the other term, so that

$$C(z) = \tfrac{1}{2} Q\chi_0^2 \ln R_m^{\frac{1}{2}} dp/dz. \tag{4.31}$$

This expression gives the contribution of $\tilde{\psi}_c$ to the vertical velocity on the axis, which is independent of r. Since the vertical velocity corresponding to $\tilde{\psi}_p$ can only be of order Q, (4.31) gives the leading-order correction $f_1(z)$ to f_0 due to the magnetic field; hence $f(z)$ can be determined as a function of Q and R_m.

4.4. *Solution for the vertical velocity $f(z)$*

From (4.31) we have $$f = f_0 + \tfrac{1}{2} Q\chi_0^2 \ln R_m^{\frac{1}{2}} dp/dz. \tag{4.32}$$

If we introduce the parameter $$\Lambda = Q\chi_0^2 \ln R_m^{\frac{1}{2}} \tag{4.33}$$

we then have $$\tfrac{1}{2}\Lambda\, dp/dz = 2zp - f_0, \quad p = 0 \quad (z = d). \tag{4.34}$$

This equation is linear in p, a pleasant surprise in such a highly nonlinear analysis; it can easily be solved to give

$$p(z;\Lambda) = \frac{2}{\Lambda} \exp(2z^2/\Lambda) \int_z^d f_0(y) \exp(-2y^2/\Lambda)\, dy = f(z)/2z. \tag{4.35}$$

The solution (4.35) is finite at $z = 0$. It can be shown that both f and d^2f/dz^2 vanish at $z = 0$, provided that f_0 and d^2f_0/dz^2 also vanish there, so that the boundary conditions (2.13a) are satisfied.

We can now indicate the conditions for the theory to be valid. It seems clear that the only condition necessary to carry through the analysis is that the flux rope be 'thin', which means that the local magnetic Reynolds number $\tilde{R}_m$ must be large. Now $\tilde{R}_m = O(R_m |p|)$ and, since $p = O(\Lambda^{-1})$ for large Λ, a necessary and sufficient condition is that $R_m \gg \Lambda$, or equivalently,

$$Q \ll R_m / \ln R_m. \tag{4.36}$$

This restriction is not very severe.

4.5. *A particular model*

The results obtained so far apply to any temperature field in (4.3). For purposes of illustration it is convenient to select a particular $\tau(r)$ that allows the problem to be

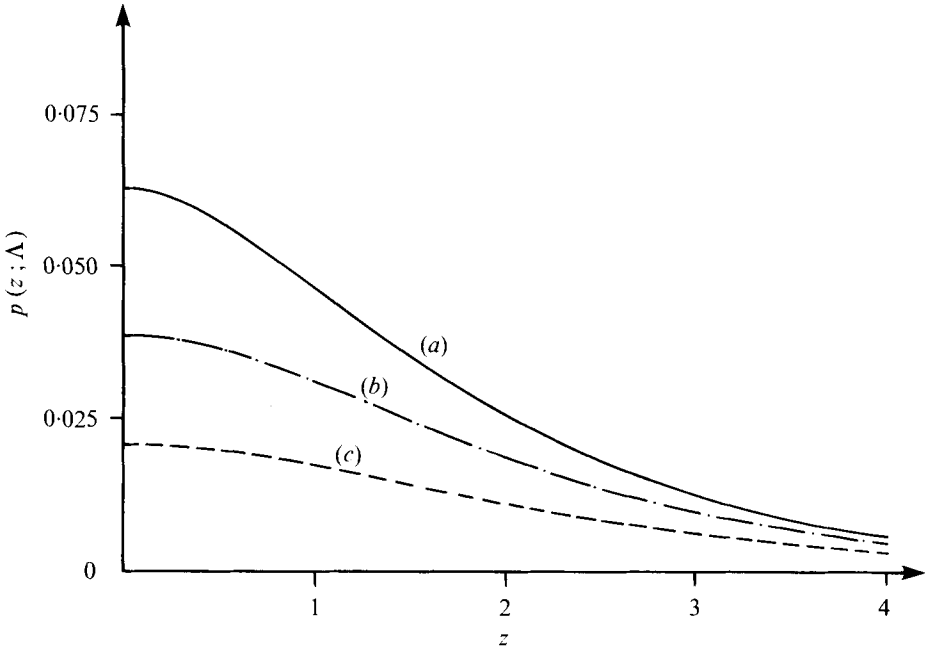

FIGURE 2. The function $p(z;\Lambda)$ (proportional to the axial field B^*) for (*a*) $\Lambda = 0$, (*b*) $\Lambda = 5$ and (*c*) $\Lambda = 20$ as a function of z.

solved exactly. If we let $d \to \infty$, choose $\tau(r) = J_0(r)$ and set $\gamma = 3{\cdot}83171\ldots$ so that $J_1(\gamma) = 0$, then

$$\theta = J_0(r)\,e^{-z}, \quad f_0(z) = \tfrac{1}{8}(z^2+z)\,e^{-z}. \tag{4.37}$$

Hence, from (4.35),

$$p(z;\Lambda) = \tfrac{1}{16}(1+z-\tfrac{1}{4}\Lambda)\,e^{-z} + \tfrac{1}{128}\Lambda^{\frac{3}{2}}\left(\frac{\pi}{2}\right)^{\frac{1}{2}} \exp\left(\frac{\Lambda}{8}+\frac{2z^2}{\Lambda}\right) \operatorname{erfc}\left[\left(\frac{2}{\Lambda}\right)^{\frac{1}{2}}\left(z+\frac{\Lambda}{4}\right)\right]. \tag{4.38}$$

In figure 2, $p(z;\Lambda)$ is plotted as a function of z for various values of Λ. We can now find the magnetic field B^* on the axis as a function of Λ. From (4.14)

$$B^*(z) = B_0 R_m\, p(z)\,\chi_0 \propto \Lambda^{\frac{1}{2}} p(z;\Lambda) \tag{4.39}$$

for fixed R_m. Now, at a given value of z, p is a decreasing function of Λ for any f_0 and, from (4.34),

$$\partial p/\partial\Lambda \sim -p/\Lambda \quad (\Lambda\to\infty), \quad \partial p/\partial\Lambda \to 0 \quad (\Lambda\to 0). \tag{4.40}$$

It follows immediately that there is a value Λ_0 of Λ, of order unity, for which

$$\partial p/\partial\Lambda + p/2\Lambda = 0.$$

But this is precisely the condition that the field B^* on the axis takes its maximum value as a function of Λ, from (4.39). The value of Λ_0 depends weakly on z; for $z = 0$ and p given by (4.38), $\Lambda_0 = 13{\cdot}5$ and the corresponding value of Q, from (4.33), is

$$Q_0 = 13{\cdot}5/(\chi_0^2 \ln R_m^{\frac{1}{2}}). \tag{4.41}$$

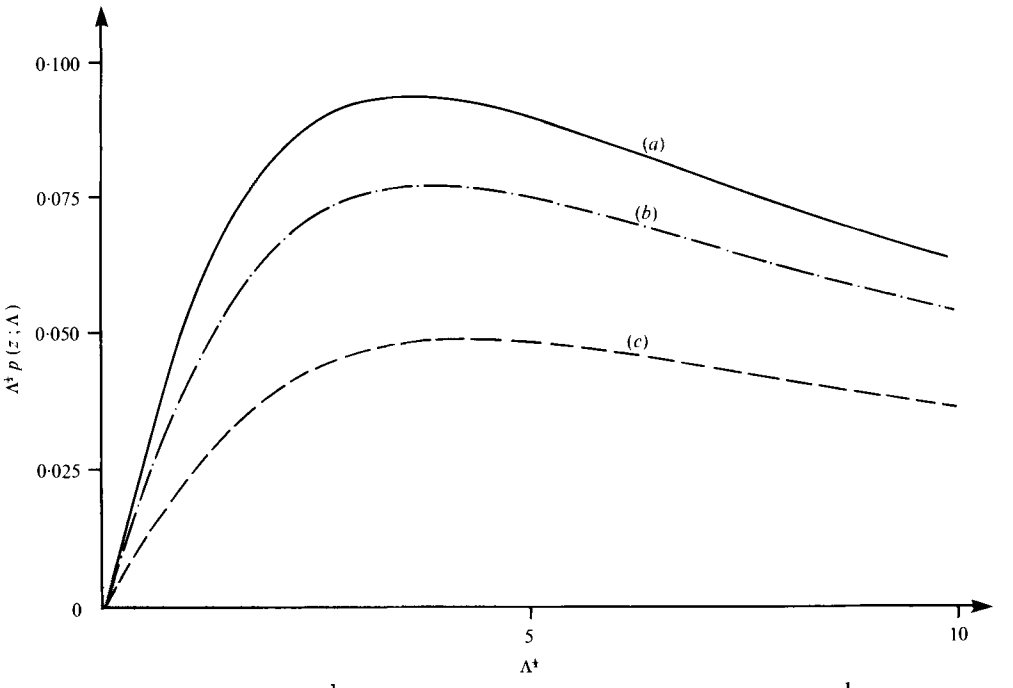

FIGURE 3. $\Lambda^{\frac{1}{2}}p(z;\Lambda)$ (proportional to B^*) as a function of $\Lambda^{\frac{1}{2}}$ (proportional to B_0) for (*a*) $z = 0$, (*b*) $z = 1$ and (*c*) $z = 2$.

So, in *dimensional* terms, the maximum value attained by B^*, at $z = 0$, is

$$B_m \doteq \frac{0{\cdot}093}{L} R_m \left(\frac{\mu\rho_0\nu\eta}{\ln R_m^{\frac{1}{2}}}\right)^{\frac{1}{2}}, \tag{4.42}$$

from (2.16) and (4.14). It follows that

$$B_m^2 \doteq 0{\cdot}017 \frac{\mu\rho_0 U^2}{\ln R_m}\left(\frac{\nu}{\eta}\right). \tag{4.43}$$

This result confirms the estimate of B_m obtained from the simplified model in § 3 and demonstrates that B^* does reach a local maximum at the transition from the kinematic to the dynamic regime. When the field is very weak, so that $\Lambda \to 0$, in the kinematic regime, $B^*(0) = \frac{1}{16}R_m B_0$ but when $\Lambda = \Lambda_0$ the ratio $B^*(0)/B_0 \doteq R_m/39{\cdot}6$. Thus the vertical velocity on the axis is reduced to about half of its value in the absence of a magnetic field; the flux rope is still thin when B^* is a maximum but the counter-velocity f_1 is comparable with f_0, as predicted in § 3. From (4.39) the amplification factor $B^*/B_0 \propto \Lambda^{\frac{1}{2}}p(z;\Lambda)$, which is plotted as a function of Λ for various values of z in figure 3. The value of Λ for which the maximum field occurs increases slowly with z, indicating that the Lorentz forces are less effective for larger values of z.

Finally, the Ohmic dissipation rate can be obtained in terms of the function p. Since the current $j = -r^{-1}D^2\chi$, the total Ohmic dissipation is given by

$$\Omega = \frac{2\pi\eta B_0^2 L}{\mu}\int_0^\infty dz \int_0^\gamma r\,dr\,.j^2 = \frac{2\pi\eta B_0^2 R_m^2 L}{\mu}\int_0^\infty p^2 dz \int_0^\infty \left[\frac{\partial}{\partial q}\left(\frac{1}{q}\frac{\partial\chi}{\partial q}\right)\right]^2 q\,dq$$
$$= \frac{\pi\eta L}{\mu}\int_0^\infty B^{*2} dz, \tag{4.44}$$

approximately. Therefore Ω, like B^*, reaches a maximum when $Q \ln R_m^{\frac{1}{2}} = O(1)$. For large values of Q

$$p = (4\Lambda)^{-1}(z^2+3z+3)\,e^{-z} + O(\Lambda^{-2}), \tag{4.45}$$

so that $B^* \sim Q^{-\frac{1}{2}}$ and $\Omega \sim Q^{-1}$ for fixed z and R_m as $Q \to \infty$. The ratio of Ω to the total viscous dissipation rate can be shown to reach a maximum of order $(\ln R_m^{\frac{1}{2}})^{-1}$ and to become very small for large Q. Thus viscous dissipation is always more important than Ohmic dissipation while the flux rope is thin.

This discussion shows the power of boundary-layer techniques in tackling the axisymmetric Oberbeck problem. The corresponding Rayleigh–Bénard problem is less tractable but yields results in the low Péclet number regime (Proctor & Galloway 1978). These thin flux rope solutions help to elucidate the vexed question of subcritical instabilities (cf. Busse 1975). Moreover, a similar treatment can be used to investigate convection in rotating systems, where $\mathbf{j} \wedge \mathbf{B}$ is replaced by $\mathbf{u} \wedge \boldsymbol{\omega}$ and the poloidal vorticity is concentrated near the axis.

5. Two-dimensional convection

The interaction between flux sheets and two-dimensional convection can be described by analogy with the three-dimensional problems with which this paper is primarily concerned. We introduce Cartesian axes with the z axis vertical and suppose that convection occurs in rolls of width L parallel to the y axis and that there is no variation in the y direction. Then the magnetic flux is concentrated into sheets in regions of rising or falling fluid between the rolls, and these sheets will be similar if the thermal boundary conditions are symmetrical.

In the kinematic regime the flux is confined to sheets of thickness ϵL, where $\epsilon \sim R_m^{-\frac{1}{2}}$, and the peak field $B^* \sim R_m^{\frac{1}{2}} B_0$. If $Re \ll 1$ the vorticity has only a y component ω which satisfies

$$\nabla^2\omega = \frac{g\alpha}{\nu}\frac{\partial T}{\partial x} - \frac{1}{\rho_0 \nu}\mathbf{B}\,.\,\nabla j \tag{5.1}$$

instead of (3.6). To estimate the maximum value of B^* we follow the procedure of § 3, scaling lengths with respect to L. First we solve the one-dimensional problem for the Green's function $\omega(x)$ given by

$$d^2\omega/dx^2 = \delta(x-\epsilon), \tag{5.2}$$

with a vertical velocity $v(x)$ and a stream function $\psi(x)$ such that $\omega = -dv/dx$, $v = d\psi/dx$ and $\psi(0) = \psi(1) = \omega(0) = \omega(1) = 0$. Then

$$V = v(0) \doteqdot -\tfrac{1}{3}\epsilon, \tag{5.3}$$

while

$$\omega = \begin{cases} 3V(1-\epsilon)\,x/\epsilon & (0 \leqslant x \leqslant \epsilon), \quad (5.4a) \\ 3V(1-x) & (\epsilon \leqslant x \leqslant 1) \quad (5.4b) \end{cases}$$

and

$$v = \begin{cases} V[1 - \tfrac{3}{2}(1-\epsilon)\,x^2/\epsilon] & (0 \leqslant x \leqslant \epsilon), \quad (5.5a) \\ V[1 + \tfrac{3}{2}\epsilon - 3x(1-\tfrac{1}{2}x)] & (\epsilon \leqslant x \leqslant 1). \quad (5.5b) \end{cases}$$

Thus the maximum vorticity $\omega^* \doteqdot 3V$ and, from (5.5), the velocity remains of the same order across the entire cell, so that $v(1) \doteqdot -\frac{1}{2}V$. The two- and three-dimensional problems have quite different solutions. The axis of a cylinder is singular; the cell boundaries are not, and so no logarithmic terms appear, while the motion extends

over the entire region instead of being confined to the vicinity of the flux rope. Moreover, the relationship between ω^* and V depends only on the cell width and not on ϵ.

The transition to a dynamic regime can be located as before. Kinematic amplification is halted when the magnetically driven counter-circulation becomes comparable with the thermally driven velocity. Hence the maximum field B_m satisfies

$$(B_m^2/\mu\rho_0\nu)\epsilon \sim U \tag{5.6}$$

and so

$$B_m^2 \sim R_m^{-\frac{1}{2}} p_2 B_e^2. \tag{5.7}$$

This field is produced when $B_0^2 \sim \mu\rho_0\nu\eta R_m^{\frac{1}{2}}$ and $Q \sim R_m^{\frac{1}{2}}$. Thus the maximum field is less than that for axisymmetric convection by a factor of order $(\ln R_m/R_m^{\frac{1}{2}})^{\frac{1}{2}}$, and occurs at a higher value of Q.

A proper two-dimensional treatment, on the lines of § 4, can be pursued for the Oberbeck problem with fluid rising into a half-space at $x = 0$ and similar boundary conditions at $x = 0$, L and $z = 0$. Once again we adopt a similar scaling and introduce a flux function χ and a stream function ψ such that $\mathbf{B} = (-\partial\chi/\partial z, 0, \partial\chi/\partial x)$ and $\mathbf{u} = (-\partial\psi/\partial z, 0, \partial\psi/\partial x)$. Then we define a stretched co-ordinate $\xi = R_m^{\frac{1}{2}} x$ for the boundary layer at $x = 0$ and assume that the stream function satisfies

$$\psi \doteq xf(z) = R_m^{-\frac{1}{2}}\xi f(z) \tag{5.8}$$

near $x = 0$. In the boundary layer the induction equation reduces to

$$\frac{\partial^2\chi}{\partial\xi^2} + \xi\frac{df}{dz}\frac{\partial\chi}{\partial\xi} - f\frac{\partial\chi}{\partial z} = 0. \tag{5.9}$$

It can be shown (cf. Proctor 1975) that this equation has a solution

$$\chi(\xi, z) = \operatorname{erf}\left\{\xi f(z)\Big/\left[\int_0^z f(\zeta)\,d\zeta\right]^{\frac{1}{2}}\right\}. \tag{5.10}$$

The corresponding velocity $\mathbf{u}_1$ can in principle be calculated by the procedure described in § 4. Inner and outer solutions $\tilde{\omega}$ and $\hat{\omega}$ may be obtained for the vorticity and the stream function $\hat{\psi}$ in the outer region satisfies the elliptic equation

$$\nabla^2\hat{\psi} = -\hat{\omega} \tag{5.11}$$

analogous to (4.26). Now the axisymmetric problem could be treated successfully because the magnetically driven flow was confined to the region near the axis, and the logarithmic term ensured that the particular integral dominated the complementary function as $r \to 0$ in (4.26). Unfortunately the velocity extends across the whole cell in two dimensions and so it becomes necessary to solve (5.11) over the entire domain and to satisfy boundary conditions at $x = 1$. The equation analogous to (4.34) for the velocity at $x = 0$ cannot be solved analytically and so there is no point in presenting all the details here.

6. Discussion

The boundary-layer analysis in § 4 demonstrated that as the average field B_0 is increased the peak field B^* remains proportional to B_0 throughout the kinematic regime and then reaches a local maximum B_m at the transition from the kinematic to

the dynamic regime. Thereafter B^* declines until the boundary-layer approximation ceases to be valid and the flux rope expands to fill the entire cell. In the Oberbeck problem, for sufficiently large Q, the field is then scarcely distorted by the motion; in the Rayleigh–Bénard problem convection is eventually suppressed. These results confirm the estimate of the maximum field B_m that was provided by the simplified model of § 3. Indeed, B_m can be estimated by dimensional arguments if the ratio of the vorticity to the velocity is known.

For the axisymmetric problem, suppose that the cell radius r_0 and the layer depth d are comparable and set $L = r_0$. Then flux is concentrated into a rope of radius $\epsilon \sim R_m^{-\frac{1}{2}} L$ at the axis. In the flux rope there is a balance between the generation of vorticity by the magnetic torque and viscous dissipation [cf. (3.6)] such that

$$\rho_0 \nu \omega_1 / \epsilon^2 \sim B^{*2} / \mu \epsilon L. \tag{6.1}$$

Now the magnetically generated vorticity ω_1 is related to the corresponding velocity v_1 by

$$\omega_1 \sim \frac{v_1}{\epsilon \ln (L/\epsilon)}, \tag{6.2}$$

from (3.13). Therefore $$v_1 \sim \frac{B^{*2}}{\mu \rho_0 \nu} \epsilon^2 \ln (L/\epsilon) \sim \frac{B^{*2} L^2 \ln R_m}{\mu \rho_0 \nu R_m}. \tag{6.3}$$

At the transition from the kinematic to the dynamic regime, when $B^* = B_m$, v_1 is comparable with U, the velocity in the absence of any magnetic field, and so

$$B_m^2 \sim \frac{\mu \rho_0 U^2}{\ln R_m} \left(\frac{\nu}{\eta}\right) \tag{6.4}$$

For specific problems the velocity U can be related to the thermal driving force, expressed in terms of the Rayleigh number defined in (2.15). Thus, from (4.1),

$$U \sim R\kappa / L \tag{6.5}$$

for the Oberbeck problem and so

$$B_m^2 \sim \frac{\mu \rho_0 \nu \eta}{L^2 \ln R_m} (p_3 R)^2 = \frac{\mu \rho_0}{\ln R_m} \left(\frac{g \alpha \Delta T L^2}{\nu}\right)^2 \left(\frac{\nu}{\eta}\right) \tag{6.6}$$

For the Rayleigh–Bénard problem at large p_1

$$U \sim R^{\frac{2}{3}} \kappa / L \tag{6.7}$$

when $R \gg 1$ (Jones *et al.* 1976); then

$$B_m^2 \sim \frac{\mu \rho_0 \nu \eta}{L^2 \ln R_m} p_3^2 R^{\frac{4}{3}} = \frac{\mu \rho_0 L^2}{\ln R_m} \left[(g \alpha \Delta T)^4 \frac{\nu}{\kappa}\right]^{\frac{1}{3}} \left(\frac{\kappa}{\eta}\right). \tag{6.8}$$

Galloway & Moore (1978) discuss power laws relating B^* to B_0 in the dynamic regime and compare them with numerical results.

Analogous arguments can be applied to two-dimensional convection in rolls of width L, where $\omega_1 \sim v_1 / L$. Instead of (6.4), we have

$$B_m^2 \sim \frac{\mu \rho_0 U^2}{R_m^{\frac{1}{2}}} \left(\frac{\nu}{\eta}\right) = \frac{\mu \rho_0 \nu \eta}{L^2} R_m^{\frac{3}{2}}. \tag{6.9}$$

For the Oberbeck problem,

$$B_m^2 \sim \frac{\mu\rho_0\nu\eta}{L^2}(p_3 R)^{\frac{3}{2}} = \mu\rho_0\left[(g\alpha\Delta T)^3\frac{L}{\nu}\right]^{\frac{1}{2}}\left(\frac{\nu}{\eta}\right)^{\frac{1}{2}}, \tag{6.10}$$

from (6.5) and (6.9) (Peckover & Weiss 1978); for the Rayleigh–Bénard problem, from (6.7) and (6.9),

$$B_m^2 \sim \frac{\mu\rho_0\nu\eta}{L^2}p_3^{\frac{3}{2}}R = \mu\rho_0 g\alpha\Delta T L\left(\frac{\kappa}{\eta}\right)^{\frac{1}{2}}. \tag{6.11}$$

From (2.2) and (2.3) it follows that the global rate of working by the buoyancy force is equal to the sum of the Ohmic and viscous dissipation rates. Obviously kinematic amplification of the field cannot persist beyond the value of B_0 for which the rate of Ohmic dissipation in the flux rope would become comparable with the overall rate of viscous dissipation in the absence of a magnetic field. Thus an upper bound to the peak field B^* can be obtained by equating the Ohmic dissipation rate Ω to the viscous dissipation rate Φ. In an axisymmetric cell

$$\Omega \sim \mu\eta j^2\epsilon d \sim \mu^{-1}\eta B^{*2}d \tag{6.12}$$

and is independent of ϵ, while $\Phi \sim \rho_0\nu U^2 d$. These two dissipation rates are equal when $B^* \sim (\ln R_m)^{\frac{1}{2}}B_m$. Thus the magnetic torque limits concentration of flux before Ohmic dissipation affects the large-scale circulation in the cell. (In fact, B^* reaches a maximum when Ω is comparable with the viscous dissipation rate for the magnetically driven flow $\mathbf{u}_1$.) In two dimensions, however,

$$\Omega \sim \mu\eta j^2\epsilon d^2 \sim \mu^{-1}B^{*2}d^2/\epsilon \tag{6.13}$$

and so $\Omega = \Phi$ when $B^* \sim B_m$: Ohmic dissipation becomes important as B^* reaches its maximum value, and convection is impeded throughout the cell. Once again, the difference between the axisymmetric and the two-dimensional configuration is caused by singular behaviour at the axis in the former. In a cylindrical cell motion can be excluded from a central flux rope without appreciably affecting the overall motion but in a two-dimensional roll the velocity is everywhere reduced.

More generally, in three dimensions, the convection cells make up a tesselated pattern. In a steady state magnetic flux is concentrated into sheets between the cells, and ropes located at their centres and their corners. We believe that almost all the flux is confined to the ropes; even if there is as much flux in the sheets as in the ropes the dynamical effect of the former is relatively unimportant (as was shown in § 5 above). Hence our results for axisymmetric flux ropes may have a much more general validity.

Unless R_m is enormous the maximum field can be adequately estimated simply by equating the viscous and Ohmic dissipation rates. We have attempted to apply this theory to the formation of intense magnetic fields in the outer layers of the sun (Galloway, Proctor & Weiss 1977). In the solar convection zone ν and η must be replaced by turbulent diffusivities $\tilde{\nu}$ and $\tilde{\eta}$; the magnetic Reynolds number $R_m = UL/\tilde{\eta}$ varies between 10^2 and 10^4 and

$$B_m \sim (\tilde{\nu}/\tilde{\eta})^{\frac{1}{2}}B_e \tag{6.14}$$

approximately. We expect that $\tilde{\eta}$, the effective diffusivity in the flux rope, is less than $\tilde{\nu}$, the eddy viscosity in the field-free region, and the fields observed in the photosphere

are indeed much greater than the local equipartition value. However, a more elaborate theory of compressible magnetoconvection is needed before these intense fields can be properly explained.

Guided by the results of numerical experiments, we have been able to describe the transition from the kinematic to the dynamic regime and to estimate the strongest fields that can be sustained by convection in a Boussinesq fluid. We expect these qualitative results to be valid in the anelastic approximation (e.g. Spiegel 1971) too. It is also possible to study fields well into the dynamic regime and appropriate power laws can be found (Galloway & Moore 1978). The nonlinear Rayleigh–Bénard problem presents formidable analytical difficulties and many features of the dynamic regime are poorly understood, but there is scope for analytical progress using the techniques developed in this paper.

We are grateful to S. Childress for encouraging us to do the boundary-layer analysis, and to G. K. Batchelor, F. H. Busse and R. S. Peckover for comments and suggestions.

REFERENCES

BATCHELOR, G. K. 1956 On steady laminar flow with closed streamlines at large Reynolds number. *J. Fluid Mech.* **1**, 177–190.

BUSSE, F. H. 1975 Nonlinear interaction of magnetic field and convection. *J. Fluid Mech.* **71**, 193–206.

CLARK, A. 1965 Some exact solutions in magnetohydrodynamics with astrophysical applications. *Phys. Fluids* **8**, 644–649.

CLARK, A. 1966 Some kinematical models for small-scale solar magnetic fields. *Phys. Fluids* **9**, 485–492.

CLARK, A. & JOHNSON, A. C. 1967 Magnetic field accumulation in supergranules. *Solar Phys.* **2**, 433–440.

GALLOWAY, D. J. 1977 Axisymmetric convection with a magnetic field. In *Problems of Stellar Convection* (ed. E. A. Spiegel & J.-P. Zahn), pp. 188–194. Springer.

GALLOWAY, D. J. & MOORE, D. R. 1978 Axisymmetric convection in the presence of a magnetic field. Submitted to *Geophys. Astrophys. Fluid Dyn.*

GALLOWAY, D. J., PROCTOR, M. R. E. & WEISS, N. O. 1977 Formation of intense magnetic fields near the surface of the sun. *Nature* **266**, 686–689.

JONES, C. A., MOORE, D. R. & WEISS, N. O. 1976 Axisymmetric convection in a cylinder. *J. Fluid Mech.* **73**, 353–388.

PARKER, E. N. 1963 Kinematical hydromagnetic theory and its application to the low solar photosphere. *Astrophys. J.* **138**, 552–575.

PECKOVER, R. S. & WEISS, N. O. 1978 On the dynamic interaction between magnetic fields and convection. *Mon. Not. Roy. Astr. Soc.* **182**, 189–208.

PROCTOR, M. R. E. 1975 Non-linear mean field dynamo models and related topics. Ph.D. dissertation, University of Cambridge.

PROCTOR, M. R. E. & GALLOWAY, D. J. 1978 The dynamic effect of flux ropes on Rayleigh–Bénard convection. Submitted to *J. Fluid Mech.*

SPIEGEL, E. A. 1971 Convection in stars I. Basic Boussinesq convection. *Ann. Rev. Astron. Astrophys.* **9**, 323–352.

SPITZER, L. 1957 Influence of fluid motions on the decay of an external magnetic field. *Astrophys. J.* **125**, 525–534.

WEISS, N. O. 1966 The expulsion of magnetic flux by eddies. *Proc. Roy. Soc.* A **293**, 310–328.

WEISS, N. O. 1975 Magnetic fields and convection. *Adv. Chem. Phys.* **32**, 101–107.

WEISS, N. O. 1977 Magnetic fields and convection. In *Problems of Stellar Convection* (ed. E. A. Spiegel & J.-P. Zahn), pp. 176–187. Springer.